New excited states in ^{168}Er: an updated analysis of the (p,t) reaction data

D. Bucurescu and S. Pascu
[1] *Horia Hulubei National Institute of Physics and Nuclear Engineering, Bucharest, Romania**

G. Graw, R. Hertenberger, H.-F. Wirth, and T. Faestermann
[2] *Fakultät für Physik, Ludwig-Maximilians-Universität München, Garching, Germany*

R. Krücken
[3] *TRIUMF, Vancouver, British Columbia, V6T 2A3, Canada*

M. Mahgoub
[4] *Physics Department, Jazan Universitym 45142 Jazan, Saudi Arabia and*
[5] *Department of Physics, Sudan University of Science and Technology, PO Box 407, Khartoum, Sudan*

J. Jolie and P. von Brentano†
[6] *Universität zu Köln, Matematisch-Naturwissenschaftliche Fakultät, Institut für Kernphysik, 50937 Köln, Germany*

R.F. Casten
[7] *Wright Lab, Yale University, New Haven, Connecticut, 06520 USA*

(Dated: February 14, 2023)

More than 200 states up to 4.1 MeV excitation have been populated in ^{168}Er with the ^{170}Er(p,t) reaction at 25 MeV incident energy. About 80 of these states, with 0^+ and 2^+ assignments, were reported in a previous publication (Phys. Rev C 73, 064309(2006)). The present work considerably enriches the knowledge of this nucleus. A multistep coupled-channel analysis of the angular distributions is now presented for all the states observed in this experiment. Spin and parity values between 0^+ and 7^- are newly assigned for more than 100 states. For the states already reported in the ENSDF database with J^π values there a good ageement with our values. The ^{168}Er nucleus remains one of the best experimentally known nuclei for states with low and medium spins below 4 MeV excitation energy, representing a challenge for future structure microscopic model calculations aiming to disentangle the contributions of different excitation degrees of freedom.

I. INTRODUCTION

The direct transfer nuclear reactions represent an important source of information on the nuclear structure. When performed with high-energy resolution, one may identify a large number of excited states with low to medium spins in nuclei, and even uniquely determine their spin and parity. Many such studies were performed at the MLL (Maier-Leibnitz Laboratory of LMU Munich and TU Munich) MP tandem accelerator using a Q3D magnetic spectrograph and a good position-sensitive focal plane detector [1–7]. A campaign of (p,t) reaction experiments was initiated in 2005 with a study of eight nuclei in the rare earth region. The main interest at that moment was to identify the 0^+ states in these nuclei, easy to recognize due to their strong forward peaking, and corroborate their distribution in excitation energy with the quantum phase transition from this region [1, 2].

^{168}Er made part of this set of nuclei, and results concerning the identification of 0^+ and 2^+ states up to 4.0 MeV excitation were published soon after these first papers, with an attempt to understand the large number of observed such states based on different theoretical models [3]. The number of states assigned as 0^+ and 2^+ was more than 80, representing less than half of all the excited states that were observed in this study, i.e. more than 200. A more detailed analysis of these data was meanwhile performed, and results concerning the assignment of a large number of states with spins between 1 and $7\hbar$ are reported in this paper. These results considerably enrich the number of low-lying states with known spin-parity in this nucleus.

II. EXPERIMENTAL DETAILS

The experiment was performed at an incident energy of 25.0 MeV. Angular distributions were measured at 7 angles between 5° and 37.5° in the laboratory system. All experimental details are given in our previous work [3]. A number of 213 excited states were observed up to an excitation energy of 4.075 MeV, with an average energy resolution of around 6 keV. The measurements at each angle were performed with three different settings of the magnetic field of the Q3D spectrograph, in such a way that the resulting spectra had an overlap in energy: 0 to 1.53 MeV, 1.4 to 2.95 MeV, and 2.5 to 4.08 MeV. The energy calibration of the spectra was achieved

* Electronic address: bucurescu@nipne.ro
† deceased

by comparing with spectra measured under similar conditions for the ^{172}Yb(p,t) and ^{208}Pb(p,t) reactions (see [3]). Most of the finally adopted excited states were observed in the energy spectra measured at all seven angles, allowing the measurement of meaningful angular distributions.

III. ANALYSIS OF THE ANGULAR DISTRIBUTIONS

To determine the transferred angular momentum (L) and spin ($J = L$) of a state populated through the (p,t) reaction, the shape of its experimental angular distribution is compared with that calculated with the code CHUCK3 [8]. The optical model potentials that describe each channel of our reaction are specified in Ref. [3]. The binding energies and the reaction Q-value are supplied, and the binding energies of the transferred two neutrons are calculated such as they match the energies of the tritons for each state. The CHUCK3 code is able to calculate both one-step processes (from the initial state directly to the final state) by using the distorted-waves Born approximation (DWBA) - in which the scattering problem is solved to first order in the interaction potential, but also by coupled-channel (CC) calculations, in which the final state can be reached by intermediate states (multistep processes) - in this case the solution of the coupled equations related to the involved states is solved to all orders of the interaction potential.

The assignment of 0^+ and 2^+ states to a number of states in Ref. [3] was performed based on DWBA (one-step) calculations. The angular distributions for the transfer of one pair of neutrons coupled to spin 0 may depend on the transfer configurations, that is, the orbitals from which these two neutrons are taken out. In principle, the real transfer may involve contributions of more than one (j_1, j_2) neutron pair (where j_i denotes the spin of the orbital), depending on the microscopic structure of the involved states. In our case, the transferred neutrons have been considered as originating from the occupied orbitals near the Fermi surface, which are mainly $2f_{7/2}$, $1h_{9/2}$ and $1i_{13/2}$ (above $N = 82$) and also from the completely filled $1h_{11/2}$ orbital (below $N = 82$).

The microscopic structure of the involved states is not known, but DWBA calculations have shown that the shape of the calculated angular distribution does not strongly depend on the considered j values of the transferred pair. This was explicitly shown for the $L = 0$ and $L = 2$ (0^+ and 2^+ states, respectively) for different (j^2) neutron pairs in ref. [3], and for $L = 0$, 2, 4 in Ref. [4]. Consequently, the L value of analysed states was assigned by recognizing the similarity of the experimental angular distributions with calculated ones. This process was the easiest for the 0^+ states, which have as unique features a strong peaking in the forward direction and a deep minimum around 14° – 17°. Similarly, the 2^+ states show a maximum around 15° and a minimum around 30° [3]. The DWBA calculated angular distributions show relatively stable shapes with characteristic maxima and minima for different other J^π values, as it will be discussed later. These structures also gradually change with the excitation energy of the final state.

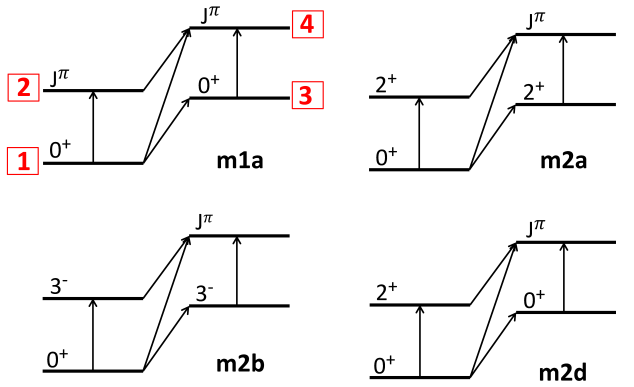

FIG. 1. Coupling schemes used in the CHUCK3 multistep coupled channels calculations (in the notation of [6]). For the "m1a" scheme, we also give the numbering of the four states used for references in the text. See also Table I for assignments of these coupling schemes to particular levels.

For many states one could assign L-values by recognizing these patterns even if they were not perfectly displayed by the experimental data. However, there are also cases when the experimentally observed angular distributions (for states of known J^π) show considerable differences from the calculated ones. These may be related to the presence of multistep excitations, which can be taken into account by performing CC calculations with CHUCK3. Such an approach was demonstrated as very useful for the ^{230}Th nucleus [4], ^{228}Th [5], ^{158}Gd [6], as well as for the ^{166}Er nucleui [7].

One may imagine many ways of coupling the initial state to the final state in the (p,t) reaction by multistep processes. Such examples of coupling schemes, which combine one-step with two-step processes, are given in [4]. Similarly to the one-step excitation, the way the two states are coupled to each other may depend on their microscopic structure. However, one finds also in this case a certain stability of the shape of the calculated angular distribution, which allows to recognize the $L(J)$ value of a certain state.

In the case of the present ^{170}Er(p,t)^{168}Er reaction, we find, like in Ref. [6], that the four coupling schemes shown in Fig. 1 are sufficient to characterize practically all the observed experimental angular distribution shapes. The population of final states (in ^{168}Er) is achieved by coupling inelastic and direct transfer channels: $(p, p') \rightarrow (p, t) \rightarrow (t, t')$. The best description of a given angular distribution shape by the calculations is obtained by adjusting the values of the amplitudes required by the code for each branch (step) of the coupling scheme. In our approach these amplitudes were taken relative to the one of the direct (one-step) coupling.

IV. RESULTS OF THE ANALYSIS

We have performed an analysis of all the states that were not considered in the former publication [3] and have a meaningful number of measured angles, and re-analysed some of the 0^+ and 2^+ states assigned in [3]. The results of this analysis are given in Table I, where the states adopted in the ENSDF database are also shown [9]. The one-step DWBA calculations are labeled by 1sdw.ij, with (ij) denoting the transfered neutron orbital configurations, while the multistep coupled-channels calculations are specified by the label of the used coupling scheme. As many of the states with 0^+ and 2^+ assignments from [3] were adopted by ENSDF, there is some repetition of this information, which appears in both columns 2 and 4. The new J^π information is given in column 5.

By looking in Table I, one can find that for a large number of states the present analysis agrees with the J^π values previously determined from other experiments [9], sometimes even suggesting a firm assignment instead a tentative one. These agreements corroborate the validity of the CC approach with the CHUCK3 code. Another general observation is that most of the known states of unnatural parity were not observed in this study (Table I). This could be explained by the fact that the unnatural parity states can be populated only by two step excitations, unlike the natural parity ones that can be excited by direct (one-step), two-step, or both these types of excitations.

TABLE I: Energy levels of ^{168}Er from the (p,t) reaction experiment, compared to the levels adopted in ENSDF [9]. The ENSDF levels are given in columns 1 and 2. Only levels with spin less than $8\hbar$ are shown. The levels previously assigned as 0^+ and 2^+ [1, 3] are shown in columns 3 and 4, but they appear also in columns 1 and 2 because they were adopted by ENSDF. All the other levels from the present analysis are given in columns 3 and 5. Column 6 gives the differential cross-section measured at 10° for all levels observed in the (p,t) reaction and column 7 the cross-section integrated over the available angular range (usually 5° to 37.5°, see the angular distribution figures). The last column gives the coupling scheme used for the CHUCK3 calculations (see Fig. 1). The one-step DWBA calculations are labeled by 1sdw.ij, with (ij) denoting the transfered neutron orbital configurations (f: $f_{7/2}$; h: $h_{11/2}$, and h9 for $h_{9/2}$; i: $i_{13/2}$), while the multistep coupled-channels calculations are specified by the label of the used coupling scheme (Fig. 1) followed by the (ij) configuration. Figures 2 to 6 show the angular distributions in the (p,t) reaction of all the levels analysed in the present work (not all the levels firmly assigned as 0^+ and 2^+ in the previous work [3] were included in the present analysis.)

ENSDF Ref. [9]		^{170}Er(p,t)^{168}Er exp.					Obs.
Energy [keV]	J^π	Energy [keV]	J^π Ref. [3]	J^π (present)	dσ/dΩ(10°) [μb/sr]	$\sigma_{\text{integr.}}$ [μb]	
0.00	0^+	0.1 *1*	0^+		584 *7*	270 *5*	
79.804 *1*	2^+	79.8 *1*	2^+	2^+	155 *4*	64 *2*	m1a.ff
264.0888 *14*	4^+	264.1 *1*	4^+	4^+	47 *1*	39.8 *7*	m1a.ff
548.7470 *20*	6^+	548.7 *1*	6^+	6^+	3.3 *2*	3.6 *2*	m2a.ii
821.1685 *16*	2^+	821.2 *1*	2^+		27.6 *4*	14.9 *4*	
895.7947 *17*	3^+	895.8 *2*		3^+	0.7 *1*	1.9 *1*	m2a.ii
928.3020 *25*	8^+	-					
994.7474 *16*	4^+	994.5 *2*		4^+	19.3 *4*	15.5 *4*	m1a.ff
1094.0383 *16*	4^-	-					
1117.5703 *16*	5^+	-					
1193.0251 *17*	5^-	1193.0 *2*		5^-	5.4 *2*	6.2 *3*	1sdw.fi
1217.169 *14*	0^+	1217.1 *1*	0^+		7.9 *2*	5.6 *3*	
1263.9047 *19*	6^+	1264.0 *1*		(6^+)	1.8 *1*	1.2 *1*	m2a.ii
1276.2716 *20*	2^+	1276.3 *1*	2^+		3.0 *2*	1.9 *2*	
1311.4606 *17*	6^-	-					
1358.899 *5*	1^-	1358.7 *2*		1^-	2.6 *1*	2.0 *2*	m2b.hi
1403.7357 *23*	$(2)^-$	1402.6 *7*		2^-	0.1 *1*	0.4 *1*	m2b.ff
1411.0959 *18*	4^+	1409.9 *8*		4^+	0.2 *1*	0.3 *1*	m1a.ff
1422.12 *3*	0^+	1421.9 *2*	0^+		5.9 *3*	4.0 *3*	

TABLE I: Continuation

ENSDF Ref. [9]		^{170}Er(p,t)^{168}Er exp.					Obs.
Energy [keV]	J^π	Energy [keV]	J^π Ref. [1, 3]	J^π (present)	dσ/dΩ(10°) [μb/sr]	$\sigma_{\rm integr.}$ [μb]	
1431.466 *4*	3^-	1431.5 *3*		3^-	9.7 *2*	9.0 *4*	1sdw.fi
1432.9508 *23*	7^+	-					
1448.9555 *17*	7^-	1448.7 *2*		(7^-)	2.9 *1*	5.1 *2*	m2b.fi
1493.133 *5*	2^+	1493.0 *2*	2^+		5.4 *2*	3.4 *2*	
1541.5564 *18*	3^-	1541.7 *5*		3^-	0.6 *1*	0.4 *1*	m2a.fi
1541.7094 *24*	$(4)^-$	-					
1569.4527 *25*	$(2)^-$	-					
1574.117 *4*	5^-	1574.0 *4*		5^-	3.3 *1*	4.7 *2*	1sdw.fi
1605.8503 *23*	8^-	-					
1615.3420 *18*	4^-	-					
1616.8060 *19*	6^+	1617.7 *5*		$(1^- + 6^+)$	1.2 *1*	0.8 *1*	doublet, 1sdw.hi,1sdw.ii
1624.507 *4*	8^+	-					
1629.698 *6*	$4^-, 5^-, 6^-$	-					
1633.4627 *23*	3^-	1633.4 *2*		3^-	11.9 *5*	11.1 *5*	1sdw.fi
1653.5486 *21*	3^+	-					
1656.274 *5*	$(4)^+$	1654.7 *5*		4^+	1.0 *1*	1.5 *1*	m1a.ff
1707.9929 *17*	5^-	1708.1 *5*		5^-	0.7 *1*	1.0 *1*	1sdw.fi
1719.1786 *24*	4^-	1718.5 *8*		(4^-)	0.4 *1*	0.3 *1*	m2b.ff
1736.6881 *20*	4^+	1736.7 *2*		4^+	10.7 *2*	10.6 *3*	1sdw.ff
1760.760 *3*	$(6)^-$	-					
1764.0 *4*		-					
≈1768.17		-					
1773.205 *3*	$(6)^-$	-					
1780.00 *15*	9^-						
		1780.3 *4*		6^+	0.8 *1*	1.3 *2*	m2a.ii
1786.123 *14*	1^-	1786.4 *3*		(1^-)	1.4 *1*	1.5 *2*	m2b.hi
1795.325 *11*	(7^-)						
		1795.4 *3*		(5^-)	0.9 *1*	1.2 *1*	m2b.fi
1812.5 *16*	$(2^+, 3, 4^+)$	-					
1820.1321 *18*	6^-	-					
1820.476 *3*	5^-	1820.5 *3*		(5^-)	2.5 *1*	2.0 *1*	m2b.hi
1828.0639 *20*	3^-	-					
1833.54 *11*	0^+	1833.7 *2*	0^+		4.9 *2*	2.4 *2*	
1839.3474 *20*	5^+	-					
1848.354 *4*	2^+	1848.2 *2*	2^+		3.1 *1*	2.3 *2*	
1881.82 *3*		-					
1892.9346 *20*	(4^-)	-					
1893.100 *6*	2^+	1893.0 *2*	2^+		1.7 *1*	1.1 *1*	
1896.379 *3*	$(7)^-$	-					
1902.696 *7*	(6^+)	1902.7 *4*		(6^+)	0.6 *1*	0.9 *1*	m2a.ii
1905.0922 *25*	(4^-)	-					
1913.92 *3*	3^-	1913.6 *3*		3^-	1.3 *1*	1.7 *1*	1sdw.fi
1915.502 *4*	$(3)^+$	-					
1930.391 *4*	2^+	1930.1 *3*	2^+		0.5 *1*	0.4 *1*	
1936.596 *10*	1^-	1936.2 *6*		1^-	1.0 *1*	0.6 *1*	1sdw.hi
1949.636 *3*	$(6)^-$	-					
1950.8067 *20*	7^-	-					
1952.2 *7*	2^+	1952.2 *7*	2^+		0.8 *1*	0.8 *1*	
1961.3992 *20*	6^+	1960.6 *5*		(6^+)	1.0 *1*	1.0 *1*	m2a.ii
1972.314 *14*	$(2)^-$	-					
1983.0398 *24*	5^-	1982.4 *4*		5^-	0.4 *1*	0.7 *1*	m2b.hi
1994.821 *4*	$(3)^+$	-					
1999.2239 *22*	$(3)^-$	-					

TABLE I: Continuation

ENSDF Ref. [9]		^{170}Er(p,t)^{168}Er exp.					Obs.
Energy [keV]	J^π	Energy [keV]	J^π Ref. [1, 3]	J^π (present)	dσ/dΩ(10°) [μb/sr]	$\sigma_{\text{integr.}}$ [μb]	
2001.953 *4*	5^-	2001.6 *3*		$3^- + 5^-$	1.2 *1*	1.5 *7*	doublet, 1sdw.fi
2002.465 *4*	$(4)^+$	-					
2022.358 *21*	$(3)^-$	2022.3 *3*		3^-	0.6 *1*	0.8 *1*	1sdw.fi
2031.097 *7*	$(4)^+$	-					
2038.66 *20*	(8^-)	-					
2055.914 *8*	$(4)^+$	2055.8 *3*		4^+	1.9 *1*	2.4 *2*	1sdw.ff
2059.9751 *20*	$(4)^-$	-					
2080.457 *3*	$(4)^+$	2080.1 *4*		4^+	1.0 *1*	1.2 *1*	m1a.ff
2089.348 *3*	4^-	-					
2091.272 *5*	$(6)^-$	-					
2097.571 *6*	4^-	-					
2100.361 *4*	7^+	-					
2108.987 *4*	$(5)^+$	-					
2114.1 *4*	0^+	2114.1 *4*	0^+		1.3 *1*	0.7 *1*	
2118.791 *5*	$(6)^-$	-					
2122.428 *3*	$(5,6,7)^-$	-					
2125.427 *4*		-					
2129.246 *21*	$(5)^-$	2129.8 *23*		–	∼0.2	∼0.2 *2*	
2133.767 *15*	(1^+)	-					
2135.9 *7*	1^-	-					
2137.08 *9*	$(2)^+$	-					
2144.53 *3*		-					
2148.3685 *23*	5^-	2148.5 *7*		5^-	0.2 *1*	0.2 *1*	m2b.fi
2169.516 *12*	$(5)^+$	-					
2174.59 *8*		2174.0		(6^+)	1.0 *1*	1.0 *1*	m2a.ii
2177.79 *8*	(2^+)	-					
2185.11 *3*	$(5)^-$	2185.5 *3*		5^-	1.5 *2*	2.5 *2*	1sdw.fi
2186.741 *4*	$(3)^+$	-					
2188.408 *10*	(5^+)	-					
2188.74 *16*	$(2^+, 3, 4^+)$	-					
2193.19 *4*	2^+	2193.0 *3*	2^+		12.2 *3*	9.2 *3*	
2200.4193 *23*	$(5)^-$	-					
2200.6 *4*	0^+	2200.6 *4*	0^+		0.4 *2*	0.4 *1*	
2210.016 *6*	(7^-)	-					
2218.5 *16*		-					
2221		-					
2230.30 *4*	$(2)^-$	2232.2 *3*		2^-	0.8 *1*	1.4 *2*	m2b.ff
2238.179 *3*	$(4)^+$						
		2238.1 *5*		1^-	1.3 *1*	1.0 *2*	m2b.hi
2243.514 *19*	$(3)^+$	-					
2246.530 *9*	$(6)^+$	-					
2249.68 *5*		-					
2254.754 *24*	(2^+)	-					
2254.84 *5*	$(3)^+$	-					
2255.343 *3*	$(6)^-$	2255.6 *5*		6^-	1.1 *1*	2.5 *2*	m2b.h9h9
2262.691 *7*	$(3)^-$	2262.8 *3*		3^-	1.9 *2*	2.4 *2*	1sdw.fi
2264 *4*	(0^+)	-					
2267.632 *8*	$(3,4,5)^+$	-					
2269 *5*	3^-	-					
2270.46 *5*		-					
2273.67 *9*	$(2^+, 3, 4^+)$						
2279.630 *5*	$(4)^+$	2279.5 *3*		4^+	1.5 *1*	1.4 *2*	m1a.ii
2286 *5*		-					
2294.0 *10*		-					

TABLE I: Continuation

ENSDF Ref. [9]		^{170}Er(p,t)^{168}Er exp.					Obs.
Energy [keV]	J^π	Energy [keV]	J^π Ref. [1, 3]	J^π (present)	dσ/dΩ(10°) [μb/sr]	$\sigma_{\text{integr.}}$ [μb]	
2298.260 *4*	$(4,5,6)^+$	2299.2 *4*		(5^+)	0.4 *1*	1.0 *1*	m2a.h9h9
2302.666 *4*	$(3)^-$	-					
2303.10 *3*	$(6)^-$	-					
2306.882 *24*	(6^+)	-					
2311.07 *3*	$(4)^+$	2311.2 *3*		4^+	3.9 *2*	4.7 *2*	1sdw.ff
2322.2 *2*	2^+	2322.2 *2*	2^+		9.6 *3*	7.9 *3*	
2323.01 *5*	3^-	-					
2331.987 *3*	6^-	-					
2336.26 *10*	4^+	-					
2337.100 *20*	3^-	2337.4 *2*		3^-	11.4 *3*	10.2 *3*	m2d.fi
2341.78 *24*	1	-					
2346.20 *9*	$1^-, 2^-, 3^-$	-					
2348.581*18*	4^-	-					
2349.3 *3*		2349.3 *3*	2^+		20.3 *4*	11.6 *3*	
2361.40 *19*	1		-				
2365.196 *14*	$(5)^-$	-					
2365.33 *12*	(1^+)	-					
2366.2 *2*	0^+	2366.2 *2*	0^+		13.4 *3*	4.9 *3*	
2368.585 *9*	(5^+)	-					
2373.657 *18*	2,3	2373.9 *6*		(1^-)	1.24 *17*	1.0 *2*	m2b.hi
2378.12 *8*		-					
2382.587 *4*	(2^+)	-					
2392.1 *2*	(0^+)	2392.1 *2*	(0^+)	0^+	3.7 *2*	2.5 *2*	m2a.h9h9
2392.118 *7*	$(5, 6^+)$	-					
2392.927 *9*	$(3^-, 4^+)$	-					
2393.71 *9*	(2^+)	-					
2398.52 *9*	$(3^+, 4, 5^+)$	-					
2401.94 *24*	(1^-)	-					
2402.29 *7*	(4^-)	-					
		2405.5 *5*		6^+	1.5 *1*	2.5 *2*	m2a.ii
2411.795 *25*	$(5)^+$	-					
2417.02 *20*	$1^{(-)}$	2416.8 *7*		–	0.8 *1*	0.4 *2*	
2423.25 *9*		-					
2424.91 *6*	$(2)^+$	2424.1 *3*		(2^+)	8.2 *3*	7.1 *3*	m1a.ff
2427.2 *6*		-					
2434.659 *5*		-					
2440.054 *20*	$(4^+, 5^+)$	-					
2440.46 *5*	(2^+)	-					
2450.5 *3*	2^+	2450.5 *3*	(2^+)		4.2 *2*	4.1 *2*	prob. doublet
2451.165 *24*	(5^-)	-					
2455.96 *6*	$(3^+, 4, 5^+)$	-					
2458.7 *4*	1	-					
2461.8 *2*	2^+	2461.8 *2*	2^+		4.9 *2*	3.7 *2*	
2468.8 *9*		-					
2474.10 *6*	(6^-)	-					
2477.20 *6*	$(5)^-$	2477.5 *3*		(5^-)	7.7 *3*	10.8 *3*	m2b.h9i
2478.08 *7*	$(3)^-$	-					
2484.52 *6*	(3^+)	-					
		2485.9 *4*		(5^-)	4.3 *3*	6.9 *3*	m2b.hi
2486 *5*	3^-	-					
		2492.2 *5*		–	1.9 *2*	2.1 *3*	
2493.5 *3*	1^+	-					
2494.528 *15*	$(3)^-$	-					
2499.1 *5*		-					

TABLE I: Continuation

ENSDF Ref. [9]		^{170}Er(p,t)^{168}Er exp.					Obs.
Energy [keV]	J^π	Energy [keV]	J^π Ref. [1, 3]	J^π (present)	dσ/dΩ(10°) [μb/sr]	$\sigma_{\text{integr.}}$ [μb]	
2510.72 *24*	$1^{(-)}$	2511.1 *4*		1^-	1.2 *1*	1.0 *2*	m2b.hi
2513.67 *5*	$(4)^-$	-					
2517.48 *20*	$(3^+,4^+)$						
		2518.5 *6*		3^-	0.4 *1*	0.6 *1*	1sdw.fi
2526.583 *12*	$(5)^-$	2526.9 *4*		(5^-)	1.9 *2*	2.5 *2*	m2b.hi
2527.78 *7*		-					
2528.80 *10*	$(5)^-$	-					
2538.1 *5*	2^+	2538.2 *5*	2^+		10.0 *3*	7.9 *3*	
2540.22 *5*	$(3,4,5)^+$	-					
2547.25 *7*	(4^+)	-					
2551.48 *7*	$(4,5)^-$	-					
2552.7 *4*	2^+	2552.3 *3*	2^+		3.0 *2*	2.5 *2*	
2558.66 *5*	$(5)^-$	-					
2561.56 *5*	(4^+)	2561.4 *2*		4^+	11.5 *3*	11.1 *3*	1sdw.ff
2563.5 *5*		-					
2571.31 *5*		-					
2572.5 *2*	0^+	2572.5 *2*	0^+		46.2 *6*	25.7 *6*	
2578.8 *5*							
		2580.4 *4*		2^+	10.8 *12*	9.4 *14*	1sdw.ff
2586.2 *6*		2585.5 *5*		1^-	1.8 *2*	1.3 *2*	m2b.hi
2594.4 *10*		-					
2601.2 *4*		-					
		2605.5 *4*		6^+	0.7 *3*	1.5 *7*	m2a.ii
2617.4 *2*	0^+	2617.4 *2*	0^+		23.6 *3*	9.4 *12*	
2626.3 *10*		-					
2628.57 *22*	$(3^+,4,5^+)$	-					
2629.2 *4*		-					
		2631.4 *4*		1^-	7.1 *2*	4.4 *5*	1sdw.hi
2637.2 *10*		-					
2643.71 *13*	$1^{(+)}$						
2644.1 *6*	(0^+)	2644.1 *6*	~~0^+~~	1^-	2.8 *2*	1.8 *3*	1sdw.hi
2651.9 *5*		2651.4 *6*		1^-	2.5 *4*	1.5 *2*	1sdw.hi
2656.86 *5*		-					
2657.66 *4*	(2,3,4)						
		2658.5 *9*		(4^+)	8.3 *4*	6.9 *5*	m1a.ff
2660.59 *7*	$(3,4)^+$	-					
2663.229 *20*	$(4)^+$	-					
2672.1 *5*	$(4^+,5,6^+)$	-					
		2673.6 *6*		5^-	1.2 *3*	3.2 *4*	m2b.hi
2676.3 *4*	1^+	-					
2683.8 *3*	(2^+)	2683.2 *4*		2^+	10.6 *2*	10.0 *4*	1sdw.ff
2689.0 *4*	$(1,2^+)$						
		2690.8 *8*		$(3^-,4^+)$	1.6 *4*	1.6 *5*	m2d.fi,m1a.ff
2694	$1^{(+)}$	-					
2700.60 *20*		-					
2703.2 *10*		-					
		2706.3 *5*		3^-	2.4 *2*	2.7 *3*	1sdw.fi
2713.2 *6*		-					
2716.0 *16*	$(2^+,3,4^+)$	-					
		2725.4 *5*		2^+	0.8 *1*	0.9 *1*	1sdw.ff
2727.77 *5*	$(4,5)^-$	-					
2728.43 *22*	1^+	-					
2733.0 *12*		2733.5 *4*		$(4^+,6^+)$	2.1 *1*	2.8 *2*	m1a.ff,m2a.ii
2738.56 *4*		-					

TABLE I: Continuation

ENSDF Ref. [9]		^{170}Er(p,t)^{168}Er exp.					Obs.
Energy [keV]	J^π	Energy [keV]	J^π Ref. [1, 3]	J^π (present)	dσ/dΩ(10°) [μb/sr]	$\sigma_{\text{integr.}}$ [μb]	
2740.16 *15*	$(4^+,5,6^+)$	-					
2740.9 *3*	1	-					
2741.9 *4*	2^+	2741.9 *4*	2^+		10.3 *4*	8.3 *5*	
2746.6 *3*	(≤ 4)	2747.6 *6*		(4^+)	5.2 *3*	4.6 *4*	m1a.ii
2751.9 *6*		-					
2757.3 *4*	$(1,2^+)$	-					
		2759 *1*		1^-	0.6 *1*	0.5 *1*	m2b.hi
2763.9 *8*	$(1,2^+)$	-					
2768.55 *6*		-					
2769.81 *15*	(5^+)	-					
		2770.2 *6*		6^+	0.8 *2*	1.5 *2*	m1a.ii
2778.03 *20*		-					
2782.9 *6*	$(1,2^+)$	-					
2786.80 *7*	$(3,4^+)$	-					
2788.1 *16*		-					
2789.2 *6*	0^+	2789.2 *6*	0^+		8.5 *2*	6.0 *6*	
2792.0 *4*	1^+	-					
2798.1 *3*	1^+	-					
2806.5 *6*		-					
		2809.2 *6*		2^+	1.9 *2*	1.8 *4*	1sdw.ff
2810.9 *4*		-					
2817.0 *4*	$(1,2^+)$	-					
2819.7 *4*		-					
2825.0 *4*	2^+	2825.0 *4*	2^+		2.3 *2*	2.2 *3*	
2826.4 *3*	$1^{(+)}$	-					
2833.7 *5*	$1^{(-)}$	-					
2842.1 *3*	0^+	2842.1 *3*	0^+		23.7 *5*	11.5 *12*	
2849.60 *5*	(4^+)	-					
2850.3 *4*	1^-	2850.4 *5*		1^-	3.7 *4*	2.9 *4*	1sdw.hi
2852.0 *5*		-					
2854.6 *4*		-					
2856.5 *6*	(2^+)	-					
		2859.1 *4*		3^-	1.4 *3*	2.1 *3*	m2a.fi
2863.6 *5*	$(1,2^+)$	-					
2872.2 *3*	0^+	2872.2 *3*	0^+		28.5 *5*	12.8 *15*	
2874.61 *3*	(3,4,5)	-					
2878.9 *4*	2^+	2878.9 *4*	2^+		5.9 *4*	5.4 *9*	
2880.6 *3*		-					
		2888.2 *5*		$(3^-,4^+)$	0.9 *2*	0.7 *2*	m2d.fi,m1a.ff
2890.65 *24*		-					
2896.7 *3*	$(3,4^+)$	-					
2901.6 *3*		-					
2906.0 *4*	2^+	2906.0 *4*	2^+		6.5 *5*	6.3 *3*	
2907.8 *3*		-					
		2915.0 *5*		6^+	5.6 *3*	8.9 *6*	m1a.ii
2920.00 *24*		-					
		2925.7 *6*		(6^+)	1.0 *4*	1.7 *2*	1sdw.ii
2929.9 *4*	$1^{(+)}$	-					
2933.44 *18*	2^+	2934.1 *5*	2^+		10.4 *3*	9.0 *4*	
2942.9 *5*		-					
2946.6 *4*	$1^{(-)}$	-					
2947.4 *4*	0^+	2947.4 *5*	0^+		48.0 *6*	22.1 *19*	
2950.7 *3*		-					
2955.6 *8*	1	-					

TABLE I: Continuation

ENSDF Ref. [9]		^{170}Er(p,t)^{168}Er exp.					Obs.
Energy [keV]	J^π	Energy [keV]	J^π Ref. [1, 3]	J^π (present)	dσ/dΩ(10°) [μb/sr]	$\sigma_{\text{integr.}}$ [μb]	
2959.1 *10*		-					
2961.2 *6*	2^+	2961.2 *6*	2^+		3.1 *2*	2.6 *2*	
2969.93 *6*	$3^+, 4^+, 5^+$	2969.3 *6*		$2^+ + 5^+$	4.0 *3*	3.9 *2*	doublet, 1sdw.ff,m2d.h9h9
2972.6 *7*	(≤ 4)	-					
2974.3 *5*	1	-					
2979.3 *3*	(≤ 4)	-					
2982.53 *10*	(3,4,5)	-					
2984.03 *23*		-					
		2987.4 *7*		1^-	1.1 *2*	0.8 *2*	1sdw.hi
2991.33 *23*	(≤ 4)	-					
2998.2 *4*	0^+	2998.3 *6*	0^+		3.5 *2*	2.5 *2*	
3002.4 *4*	($1,2^+$)	-					
3009.0 *3*	2^+	3009.0 *3*	2^+		20.7 *4*	18.2 *4*	
3011.77 *23*	(4^+)	-					
3019.6 *5*	2^+	3020.0 *5*	2^+		1.9 *2*	1.5 *2*	
3026.02 *19*		-					
3028.6 *6*	0^+	3028.6 *6*	0^+	0^+	5.1 *2*	4.0 *2*	1sdw.ii
3030.7 *5*		-					
3033.9 *5*	(≤ 4)	-					
3042.3 *4*	2^+	3042.4 *5*	2^+		10.7 *3*	8.0 *3*	
3042.8 *3*	$3^-, 4^-, 5^-$	-					
3044	1	-					
3049.6 *4*	1^+	-					
3049.9 *5*	2^+	3049.9 *5*	2^+		5.0 *4*	4.8 *5*	
3055.95 *23*	2^+	3055.1 *5*	2^+		1.2 *4*	1.0 *5*	
3063.6 *3*		-					
3065.0 *7*	(0^+)	3065.0 *7*	~~0^+~~	1^-	1.4 *2*	1.1 *2*	1sdw.hi
3068.8 *3*		-					
3078.0 *14*		-					
3081.3 *6*	2^+	3081.3 *6*	2^+		3.8 *3*	4.0 *4*	
3082 *1*	1	-					
3082.8 *5*	(4^+)	-					
3087.8 *4*		3087.0 *5*		2^+	0.8 *3*	0.9 *6*	1sdw.ff
3095.9 *6*	$1^{(-)}$	-					
3098.4 *6*	2^+	3098.4 *6*	2^+		2.3 *2*	2.5 *2*	
3099.42 *8*	(3^-)	-					
3106.6 *6*		-					
3111.24 *15*	($2^+, 3, 4^+$)	-					
		3112.9 *6*		(3^-)	2.0 *2*	1.4 *3*	m2d.fi
3116.4 *5*	(2^+)	-					
3116.8		3116.8 *8*	(0^+)	(0^+)	~ 0.8	1.0 *2*	m2a.ii
3118.1 *5*		-					
3124.40 *20*	(4^+)	-					
3124.5 *7*	1^+	-					
3127.93 *25*	($4^+, 5, 6^+$)	-					
3131.9 *5*		-					
3137.6 *6*		-					
3139.6 *6*	2^+	3139.6 *6*	2^+		7.0 *3*	6.2 *3*	
3142.7 *5*		-					
3147.2		3147.5 *5*	~~(0^+)~~	3^-	4.3 *3*	2.6 *2*	m2a.h9i
3151.9 *16*	(≤ 4)	-					
3157.5 *7*	0^+	3157.5 *7*	0^+	0^+	1.0 *2*	0.6 *2*	1sdw.ii
3158.3 *16*		-					

TABLE I: Continuation

ENSDF Ref. [9]		^{170}Er(p,t)^{168}Er exp.					Obs.
Energy [keV]	J^π	Energy [keV]	J^π Ref. [1, 3]	J^π (present)	dσ/dΩ(10°) [μb/sr]	$\sigma_{\text{integr.}}$ [μb]	
		3164.7 *7*		(3^-)	0.8 *2*	0.8 *2*	1sdw.fi
3172.5 *7*	2^+	3172.5 *7*	2^+		7.5 *3*	7.0 *3*	
3181.1 *6*	1^-	-					
3183.7 *8*	2^+	3183.7 *8*	2^+		12.0 *3*	11.8 *3*	
3190	1^-	-					
3194.4 *8*	2^+	3194.4 *8*	2^+		2.6 *2*	2.4 *2*	
3198.0 *16*	(≤ 4)	-					
3205.2 *16*		-					
3208.0 *8*	$1^{(+)}$	-					
		3219.9 *9*		(3^-)	1.0 *1*	1.4 *2*	m2a.hi
3220	1						
3223.2 *16*	(4^+)	-					
3237.2 *8*	2^+	3237.2 *8*	2^+		4.9 *3*	4.5 *3*	
3238.0 *16*		-					
3242.6 *8*	1	-					
		3244.2 *10*		3^-	1.6 *2*	1.4 *3*	m2d.hi
		3262.7 *12*		4^+	0.9 *2*	1.8 *2*	m1a.ff
3269.4 *8*	2^+	3269.4 *8*	2^+		1.6 *2*	0.9 *2*	
3285.1 *16*	(4^+)	-					
3286.8 *8*	2^+	3286.8 *8*	2^+		3.6 *2*	4.6 *9*	
		3294.6 *8*		$(1^- + 4^+)$	2.3 *2*	2.4 *2*	1sdw.hi,1sdw.ff
3300.0 *7*	1	-					
		3305.7 *9*		(3^-)	1.8 *2*	2.6 *2*	1sdw.fi
3312.8		3312.8 *15*	~~(0^+)~~	–	1.0 *2*	0.6 *2*	
		3319.2 *18*		–	1.1 *6*	1.3 *4*	
		3326.3 *19*		–	0.6 *5*	0.7 *4*	
3327.3 *16*	(≤ 4)	-					
3335.0 *16*	$(4^+, 5^+)$	-					
3338.2 *6*	(2^+)	-					
3342.0 *10*	$1^{(+)}$	-					
3342.9 *10*	2^+	3342.9 *10*	2^+		2.0 *2*	1.3 *2*	
3347.7 *16*		-					
3358.7 *6*	1^+	-					
3361.9 *10*	2^+	3361.9 *10*	2^+		3.8 *2*	3.9 *2*	
3370.9 *7*	(2^+)	-					
		3371.6 *8*		5^-	1.5 *2*	2.4 *2*	m2b.h9i
3376.6 *16*	(4^+)	-					
		3380.6 *8*		(0^+)	1.5 *2*	2.4 *2*	m2a.ii
3391 *1*	1^+	-					
		3391.1 *8*		2^+	0.9 *2*	1.1 *2*	1sdw.ff
3394.5 *16*		-					
3399.3 *16*	(≤ 4)	-					
		3404.9 *8*		–	1.5 *2*	1.5 *2*	
3409.7 *9*	1^+	-					
3415.5 *16*	(≤ 4)	-					
		3418.2 *10*		2^+	1.1 *2*	1.5 *2*	1sdw.ff
3429.2*10*	2^+	3429.2 *10*	2^+		5.6 *2*	5.6 *3*	
3432.0 *16*	(4^+)	-					
3439.6 *9*	$1^{(-)}$	-					
3441.7 *10*	2^+	3441.7 *10*	2^+		3.7 *2*	4.0 *2*	
3449	1	-					
3451.6 *10*	2^+	3451.6 *10*	2^+		1.9 *2*	2.5 *2*	
3458 *2*	1^+	-					
3459.9 *10*	2^+	3459.9 *10*	2^+		2.1 *2*	2.6 *2*	

TABLE I: Continuation

ENSDF Ref. [9]		^{170}Er(p,t)^{168}Er exp.					Obs.
Energy [keV]	J^π	Energy [keV]	J^π Ref. [1, 3]	J^π (present)	dσ/dΩ(10°) [μb/sr]	$\sigma_{\text{integr.}}$ [μb]	
3469 *2*	1^-	-					
3471.6 *10*	2^+	3471.6 *10*	2^+		2.5 *2*	3.1 *2*	
3475.7 *16*	(≤ 4)	-					
3481 *2*	1^-	-					
3482.6 *10*	2^+	3482.6 *10*	2^+		2.9 *2*	4.1 *2*	
3487.3 *16*		-					
3493.3 *10*	2^+	3493.3 *10*	2^+		10.0 *3*	10.8 *3*	
3496.4 *16*	(4^+)	-					
3499.3 *16*		-					
3504.2 *9*	1^-	-					
3506.3 *10*	2^+	3506.3 *10*	2^+		6.8 *2*	7.8 *3*	
3507.8 *16*	(≤ 4)	-					
3513.9 *16*		-					
3515.7 *12*	2^+	3515.7 *12*	2^+		1.9 *2*	2.5 *2*	
3516	1^-	-					
3521.1 *16*	(≤ 4)	-					
3529	1	-					
		3529.0 *10*	~~0^+~~	(4^+)	2.8 *2*	2.1 *2*	m1a.ii
		3535.0 *15*		(3^-)	0.5 *2*	1.3 *2*	m2a.hi
		3546.8 *15*		(3^-)	0.5 *1*	1.2 *2*	m2a.hi
3560.0 *16*		-					
3561.9 *12*	2^+	3561.9 *12*	2^+		2.8 *2*	2.7 *2*	
3566	1	-					
3569.4 *10*	0^+	3569.4 *10*	0^+	0^+	3.7 *2*	2.4 *2*	m2a.h9h9
3570.9 *16*	(4^+)						
		3577.4 *10*		(2^+)	3.1 *2*	2.8 *3*	m1a.ii
3581.1		3581.1 *10*	~~0^+~~	–	~ 1.7	0.3 *2*	
3586.3 *10*	0^+	3586.3 *10*	0^+	0^+	3.0 *2*	1.9 *3*	m2a.h9h9
3588.0 *16*		-					
3591	$1^{(+)}$	-					
3598	1	-					
		3599.3 *10*		2^-	0.7 *2*	1.3 *2*	m2b.ff
3606.8 *16*	(≤ 4)	-					
		3610.2 *10*		–	~ 0.6	0.3 *1*	
3617.6 *12*	2^+	3617.6 *12*	2^+		1.4 *2*	1.6 *2*	
3627	1	-					
3629.9 *12*	2^+	3629.9 *12*	2^+		1.2 *2*	1.9 *3*	
3634	$1^{(-)}$	3634.8 *10*		–	1.3 *2*	0.8 *3*	
		3642.8 *10*		(3^-)	0.6 *2*	0.8 *1*	m2a.hi
3643.1 *16*	(≤ 4)	-					
3657	$1^{(+)}$	-					
3660.9 *16*	(≤ 4)	-					
3663.9 *10*	0^+	3663.9 *10*	0^+	0^+	8.7 *2*	3.8 *2*	m2a.h9h9
		3671.6 *10*		–	2.1 *10*	1.9 *6*	
		3675.9 *10*		3^-	1.5 *3*	1.2 *4*	1sdw.fi
3680.1 *16*	$(2^+, 3, 4^+)$	-					
3682.5		3682.5 *10*	~~0^+~~	2^+	4.1 *2*	2.9 *3*	m1a.ff
3696	1						
		3696.7 *10*	~~0^+~~	(3^-)	1.3 *2*	1.1 *2*	m2d.fi
3702.5 *16*	(≤ 4)	-					
3703	1^-	-					
3714.9 *10*	(0^+)	3714.9 *10*	0^+	0^+	1.4 *2*	0.7 *2*	m2a.h9h9
3715.2 *16*		-					
3719	$1^{(-)}$	-					

TABLE I: Continuation

ENSDF Ref. [9]		^{170}Er(p,t)^{168}Er exp.					Obs.
Energy [keV]	J^π	Energy [keV]	J^π Ref. [1, 3]	J^π (present)	dσ/dΩ(10°) [μb/sr]	$\sigma_{\rm integr.}$ [μb]	
3720.0 *15*	2^+	3720.0 *15*	2^+		2.6 *2*	2.5 *2*	
3725.2 *15*	2^+	3725.2 *15*	2^+		1.4 *2*	1.4 *2*	
3734.4 *10*	0^+	3734.4 *10*	0^+	0^+	5.0 *2*	2.0 *2*	m2a.h9h9
3737	1	-					
3739.0 *16*	$(2^-, 3, 4^+)$	-					
3740.4 *15*	2^+	3740.4 *15*	2^+		2.7 *2*	2.8 *3*	
3745	$1^{(-)}$	-					
		3751.5 *15*		2^+	1.7 *1*	1.6 *2*	1sdw.ff
3755.4 *16*		-					
3760.1 *10*	0^+	3760.1 *10*	0^+	0^+	7.2 *2*	3.2 *2*	m2a.h9h9
3761.6 *16*	(≤ 4)	-					
		3768.4 *15*		(0^+)	0.8 *1*	1.0 *2*	m2a.h9h9
3776	$1^{(+)}$	-					
3781.7 *16*	$(4^+, 5, 6^+)$	-					
3789	1	-					
3789.5 *15*	2^+	3789.5 *15*	2^+		1.4 *2*	1.2 *2*	
		3794.1 *15*		2^+	0.9 *2*	1.0 *2*	1sdw.ff
3799.4 *16*		-					
3800	$1^{(-)}$	-					
3806	1^+	-					
3808.5 *15*	2^+	3808.5 *15*	2^+		3.2 *2*	2.9 *2*	
3814	$1^{(-)}$	-					
3817.0 *16*	(≤ 4)	-					
3819.4 *15*	2^+	3819.4 *15*	2^+		3.8 *2*	3.8 *2*	
		3826.4 *15*		–	0.6 *2*	1.0 *2*	
3835.2 *16*		-					
		3838.0 *15*		2^+	0.5 *2*	0.8 *2*	1sdw.ff
3861.9 *15*	2^+	3861.9 *15*	2^+		1.7 *2*	1.6 *2*	
3868.7 *15*	2^+	3868.7 *15*	2^+		4.7 *2*	5.0 *2*	
3869	1	-					
3876.3 *15*	2^+	3876.3 *15*	2^+		2.5 *2*	2.9 *2*	
3888.4 *16*		3889.1 *15*		(1^-)	1.1 *2*	0.7 *1*	m2b.hi
3895.2 *16*		-					
3908.3 *16*		-					
3912	1	-					
3921	$1^{(-)}$	-					
		3923.1 *15*		2^+	1.2 *2*	1.5 *2*	1sdw.ff
3928.9 *10*	0^+	3928.9 *10*	0^+	0^+	3.2 *3*	2.3 *3*	m2a.h9h9
3933.0 *15*	2^+	3933.0 *15*	2^+		2.1 *3*	2.1 *3*	
3960		3960.3 *15*		–	3.2 *3*	1.7 *2*	
3964.9 *15*	2^+	3964.9 *15*	2^+		1.3 *3*	3.1 *2*	
		3972.5 *15*		(3^-)	2.5 *2*	2.3 *2*	m2d.hi
3993		3992.5 *15*		3^-	5.3 *2*	6.9 *3*	m2a.hi
		4005.6 *15*		4^+	1.7 *3*	2.0 *4*	m1a.ff
		4009.0 *15*		2^+	1.5 *3*	1.9 *4*	1sdw.ff
		4020.3 *15*		(3^-)	2.0 *2*	2.1 *2*	m2d.hi
4033.5 *15*	2^+	4033.5 *15*	2^+		1.6 *2*	2.1 *2*	
		4041.9 *15*		(6^+)	0.6 *2*	1.6 *2*	m1a.ii
4055.9 *15*	2^+	4055.9 *15*	2^+		2.1 *3*	1.9 *3*	
		4060.7 *15*		2^+	1.2 *2*	1.8 *3*	1sdw.ff
4069		4069.2 *15*		2^+	0.6 *2*	0.6 *2*	1sdw.ff
4075.6 *15*	2^+	4075.6 *15*	2^+		1.9 *2*	2.2 *3*	

A. 2^+ states and 4^+ states

A number of 66 states were assigned as 2^+ in Ref. [3], based on the good description of their angular distribution by one-step DWBA calculations. For some of these

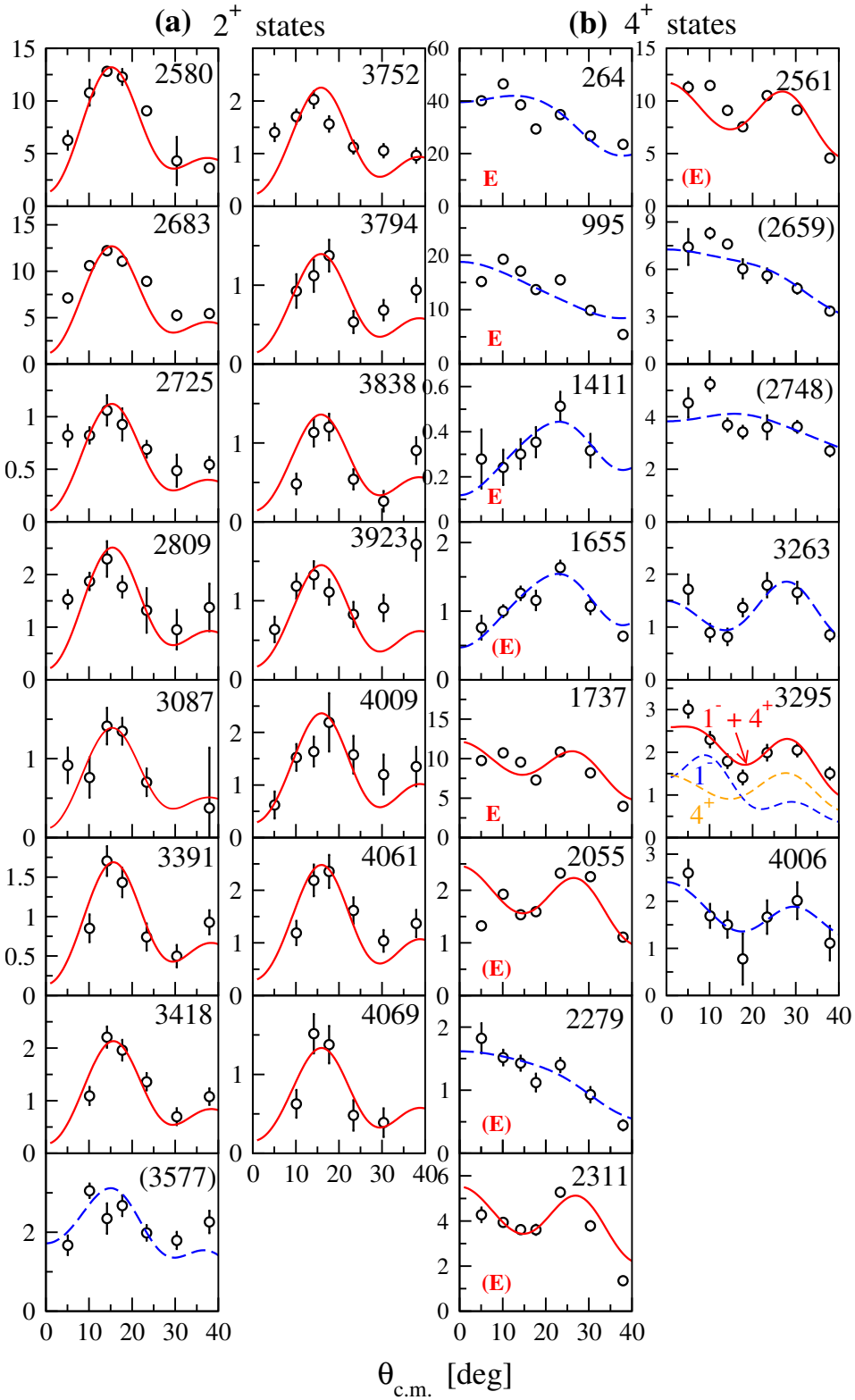

FIG. 2. Angular distributions of ^{168}Er states with (a) 2^+ and (b) 4^+ J^π assignments. Calculations with CHUCK3 are shown by curves normalized to the experimental data. The energies from Table I shown for each of the states were rounded off to the nearest keV of the more precise energy given in Table I. The continuous (red) curves are one-step DWBA calculations, while the dashed (blue) ones correspond to coupled-channel calculations with the coupling schemes specified in Table I. A label "E" or "(E)" in the lower left corner of a graph denotes a firm or tentative J^π assignment, respectively, as accepted in the ENSDF database [9] for that state (see Table I). For the states with energy within parantheses our spin assignemnt is tentative (see also Table I). For the 2^+ states only those assigned in this study at higher energies (above 2500 keV) are shown (in addition to those of Ref. [3]).

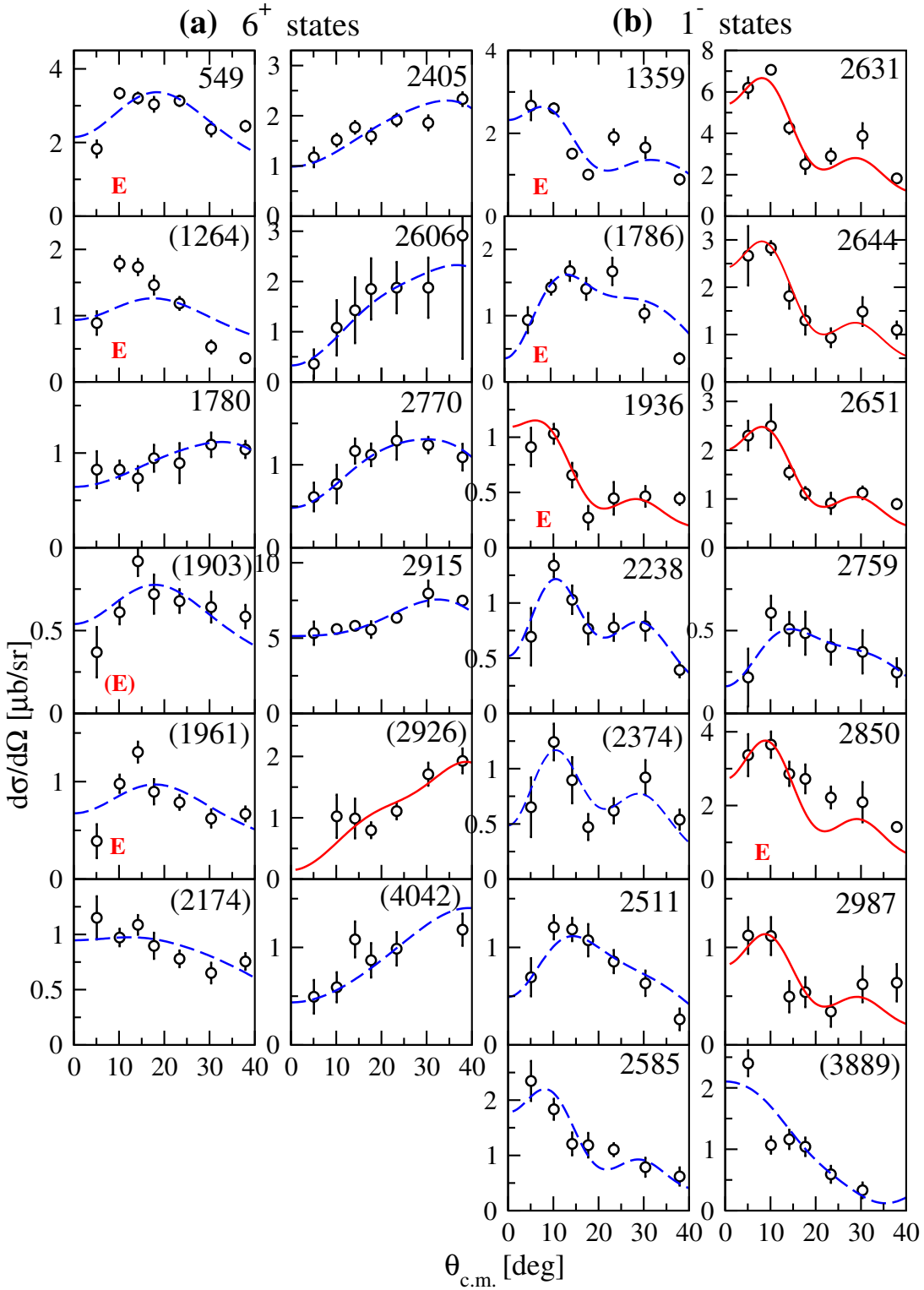

FIG. 3. The same as Fig. 2, but for the states with (a) 6^+ and (b) 1^- J^π assignments.

states, this assignment confirmed the value previously known from other sources [9]. Out of all these states, (Fig. 5 in [3]) we have only checked that the shapes observed for the states at the excitation energies of 80 keV and 2424 keV are well described by coupled channel calculations (Table I). In addition, we find a number of 15 states newly assigned as 2^+ (Fig. 2a), all above 2.5 MeV excitation, also well described by one step calculations

(except for the tentatively assigned state at 3577 keV which required a CC calculation).

For the 4^+ states, we have analysed all states, starting with the 4_1^+ state at 264 keV - Fig. 2(b). For all such states found up to 2.56 MeV excitation we have been able to confirm earlier, independent assignments [9]. In most of the cases, a coupled channels analysis was necessary to describe the observed angular distribution shape (Fig. 2). The assignment given for the 3295 keV level is only tentative, as it was found that this is maybe a doublet, the shape of which can be fitted by a combination of calculated transfers of 1^- and 4^+.

B. 6^+ states and 1^- states

Part (a) of Fig. 3 displays the states assigned as 6^+. It is interesting that the states up to 2 MeV excitation, known from previous studies as 6^+ [9] (except for that at 1780 keV) needed coupled channels calculations that considerably change the shape of the one-step calculations (see for example the curve for 2926 keV state).

Part (b) of Fig. 3 shows 1^- states. For many of them (including some with previously known 1^- assignment) the observed experimental angular distribution shows a characteristic pattern, with two maxima, at about 10° and 30°. These features show up also in some CC calculations where the two-step excitations have a smaller weight. One should also observe that the only way to calculate 1^- states is to take the neutrons from both above and below the $N = 82$ gap, because only the combination between the orbitals of opposite parities $1i_{13/2}$ and $1h_{11/2}$ can provide a spin 1 state.

C. 3^- states and 5^- states

Fig. 4(a) displays the states assigned as 3^-. Many states present a maximum at about 20° which is also a characteristic of the one-step calculations. For the first six states of lower energies one confirms the J^π previous assignment. The other states present various influences of multistep excitation mechanism.

Fig. 4(b) shows the states assigned as 5^-, for seven of them this assignment confirms the ENSDF one. Characteristic of the one-step mechanism of this excitation is the maximum around 30° which is still observed in some of the states with multistep excitation influence. The angular distribution of the peak at 2001.6 keV is fitted by a combination of $L = 3$ and $L = 5$ (calculated as one-step processes) in agreement with the known closely lying levels present around this energy (see Table I).

D. 0^+ states

Fig. 5(a) shows an analysis of some of the 0^+ states previously assigned in Ref. [3], as well as newly assigned states. Since 0^+ assignments are easy to make based on the strong forward peaking and the deep minimum around 17°, in Ref. [3] there were no special efforts to fit the angular distribution shape, but just a comparison with one step calculations for a $2\text{x}f_{7/2}$ transfer. While up to 3 MeV excitation this approach leads to rather firm assignments, above this excitation energy there is some evolution of the experimental angular distribution shape that increases the discrepancy with the calculations: One can see (Fig. 3 of Ref. [3]) that the minimum of the angular distributions at about 17° fills up, while that of the calculations is much deeper. For the states approaching 3.9 MeV excitation the assignment can even be put under question mark (even if the logarithmic scale used in that figure exacerbates the discrepancy in the zone of the minimum). We have re-analysed the states between 3 and 3.9 MeV excitation with coupled channel calculations, and succeeded to reproduce very well the evolution in the minimum region - this is shown in the first column of part (a) of the figure. In Fig. 3 of [3] there were also four other states tentatively assigned (as (0^+)): 2392, 2644, 3065, and 3715 keV. A re-analysis of these four states with CC calculations has the following results: only the states at 2392 and 3715 have a 0^+ firm assignment (they are shown in the upper part of the second column of the figure), while the states at 2644 keV and 3065 keV have now been assigned as 1^- (see 3065 keV in part (c) of this figure, and 2644 keV in Fig. 3(b)).

There were also seven states in Ref. [3] that were characterised as "possible 0^+ states", only on the basis on their relatively strong forward peaking: 3117, 3147, 3313, 3529, 3581, 3683, and 3697 keV (Fig. 4 of [3]). From the coupled channels analysis of other states discussed above, it is clear that angular distributions with such forward peaking are frequently obtained. Therefore, these seven states have been analysed with multistep CC calculations, with the following results. Only the 3117 keV state remained with a tentative (0^+) assignment (see second column of Fig. 5(a)). From the remaining six states, four of them have been assigned different J^π (see part (b) of Fig. 5), and two of them (3313 and 3581 keV) could not be given any assignment (they are shown in part (b) of Fig. 6). Oher two states with energies of 3380 and 3768 keV have been newly assigned as (0^+) states (the last two states shown in part (a) of Fig. 5).

In conclusion, we have re-confirmed as 0^+ all the states assigned as such up to 3.29 MeV excitation, only two of the four states tentatively assigned as 0^+, and only one of the seven "possible 0^+" states from the previous analysis [3], and assigned other J^π values to the rest of the states discussed in that paper. In addition, two other states were newly assigned as (0^+) states. In total, the number of states with firm or tentative 0^+ assignment from both our previous analysis and the present work is 28. In Table I, the firm or tentative 0^+ assignments from Ref. [3] of some of the states discussed above that were not confirmed by the present analysis have been crossed out (in column 4 of the table) and replaced by the new

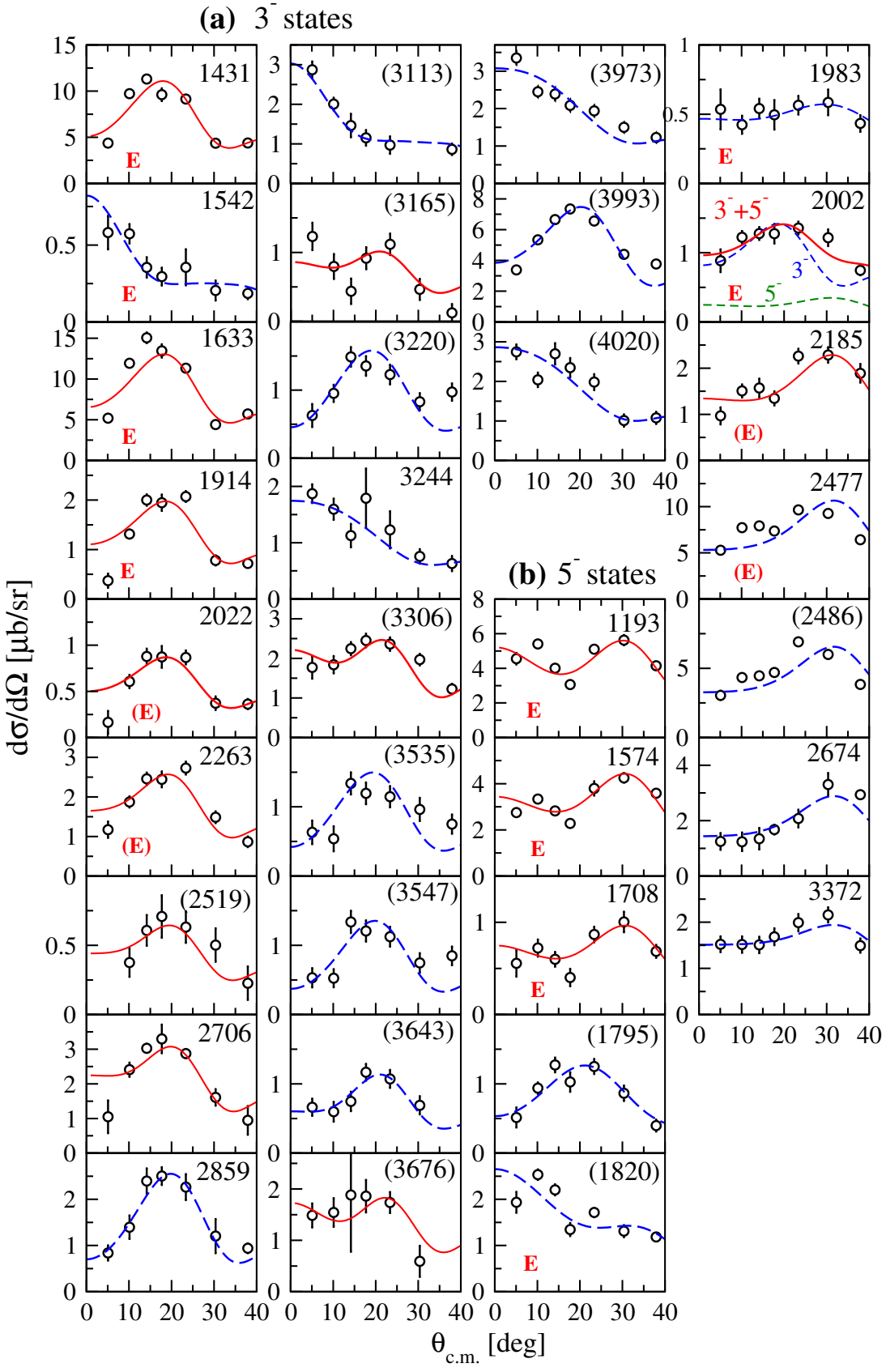

FIG. 4. The same as Fig. 2, but for the states with 3^- and 5^- J^π assignments.

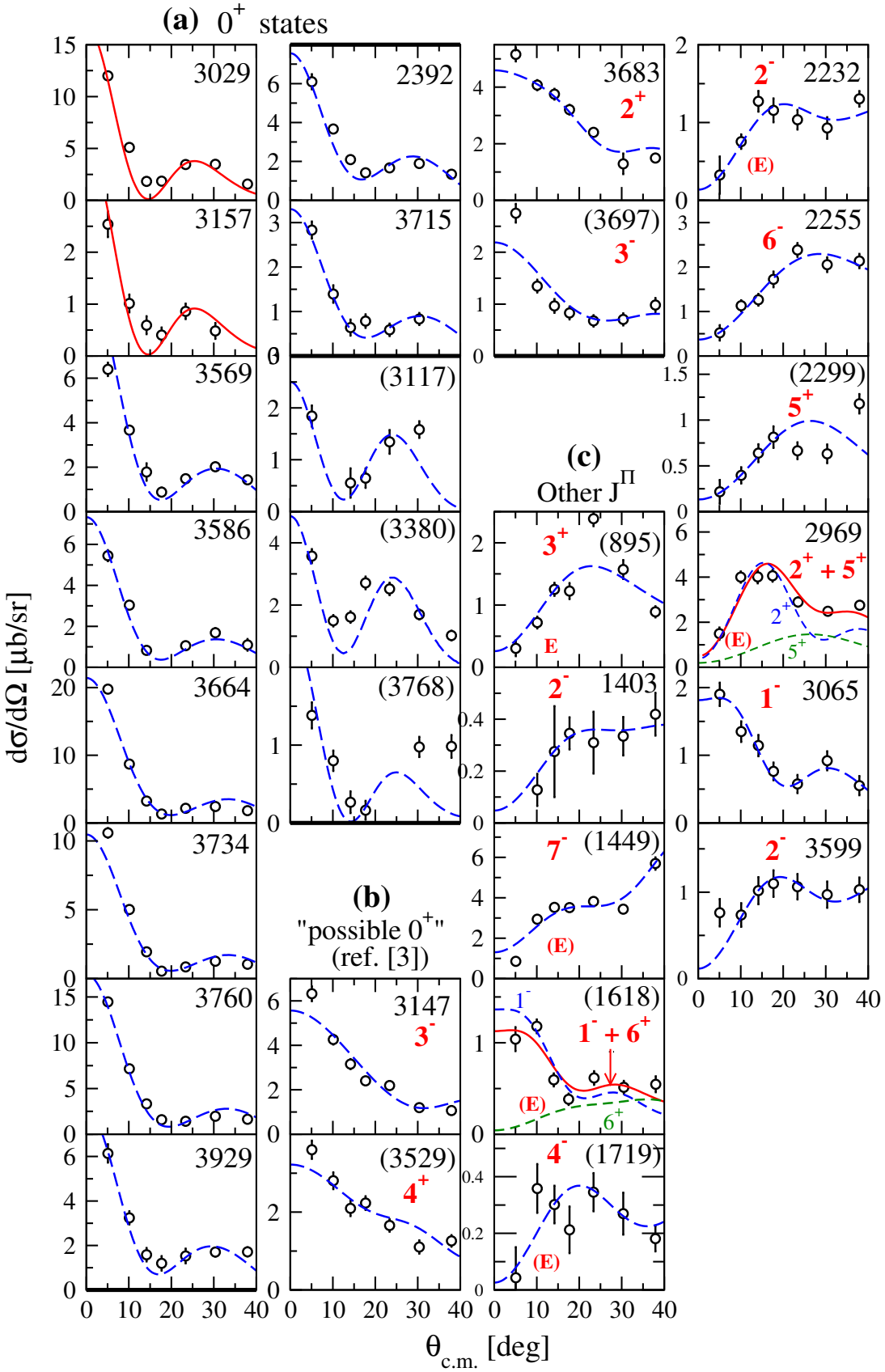

FIG. 5. Similar to Figs. 2 and 3, for states of other J^π values from this study. (a) Re-analysis of states with excitation energies between 3000 to 3950 keV previously assigned as 0^+ (Fig. 3 of [3]). The upper two graphs of the second column refer to the 2392 and 3715 keV states which had only tentative assignment [3]. Two other states also tentatively assigned as 0^+ (2644 and 3065 keV) were now assigned as 1^- (see Fig. 3 and part (c) of this figure). For the rest of three states assigned as (0^+): 3117 keV is one of a set of seven states which, due to their relatively large forward peaking were proposed as "possible 0^+ states" (Fig. 4 of Ref. [3]), while 3380 and 3768 are newly assigned. (b) Analysis of the other states from 3117 to 3697 keV proposed "possible 0^+ states" in [3]: two of the states from this category (3313 and 3581 keV) could not be assigned J^π values (see section (b) of Fig. 6), while the rest of four states were assigned as shown in part (b) of this figure. (c) Analysis of states.with other J^π values.

assignment (in column 5).

E. States with other J^π assignments

Different other J^π assignments are shown in part (c) of Fig. 5. Most of these states have unnatural parity, such as 2^-, 3^+, 4^-, and 5^+. Most of the assigned J^π values confirm the values from ENSDF [9]. The unnatural parity states have been analysed with coupling schemes from Fig. 1 which have been adapted to them. As an example, the 2^- and the 4^- states were calculated with the m2b scheme that was truncated: only the transitions channel 1 $\rightarrow$ channel 2 $\rightarrow$ channel 4 were allowed, therefore these states have been described by a pure two-step process. The 3^+ state has been analysed with the m2a scheme (Fig. 1), without the direct branch (channel 1 $\rightarrow$ channel 4). The peak at 2969 keV appears to be a doublet containing the known (5^+) state (Table I) and a 2^+ state.

F. Ambiguities of the analysis

During our analysis with the multistep coupled channels calculations we found that sometimes it was impossible to assign a single L value (or J^π) to certain angular distributions. This is illustrated for six states in part (a) of Fig. 6. This indetermination is due to the fact that one may find two or even three calculated shapes with different L-values, that are very similar (e.g., 3^- and 4^+; 5^- and 6^+; etc.). For the first four states presented in Fig. 6(a), one of the possible values indicated by our analysis coincides with the J^π value from the ENSDF, therefore we have adopted that value too (see Table I).

The similarity of angular distributions calculated for different L values is more likely to appear when the angular distribution shapes are relatively flat (have a small ratio between the maximum and minimum value). In some cases, a better definition of the experimental shape (e.g., better statistics of the points, a smoother pattern) would help choosing between the calculated curves. Nevertheless, one should be aware that an analysis with coupled channel calculations may not always be unambiguous, and for this reason in certain cases presented in the earlier subsections we adopted only a tentative J^π assignment.

G. Unassigned states

Part (b) of Fig. 6 shows the states that could not be assigned a certain J^π value in the present analysis. In some cases, the angular distribution shape was not well defined due to the small number of angles where the state was observed. In other cases, the angular distribution had large uncertainties, its shape could not be matched with any of those obtained in our trials with CC calculations, or more levels with closely lying energies mau be present.

V. DISCUSSION

More than 120 states observed in the ^{170}Er(p,t)^{168}Er reaction have been analysed for the first time, and some states discussed in the previous publication [3] were reanalysed, with multistep coupled channel calculations with the code CHUCK3. In more than 30 cases the assigned J^π values coincide with those adopted by ENSDF [9] based on experimental data from other sources. The total number of the states assigned as 0^+ and 2^+ (including those reported in [3]) are 28, and 81, respectively. The newly added states, two in the 0^+ case and eighteen in the 2^+ case, do not significantly alter the distribution in excitation energy and in population intensity discussed in [3]. In these two cases a comparison was made in [3] with the predictions of two microscopic models: the Quasiparticle-phonon model [10] and the Projected shell model [11]. Both these models predict numbers of 0^+ and 2^+ states comparable to the observed ones, at least up to $\sim$3 MeV excitation, but fail to predict details of the observed distribution of the reaction transfer strengths of these levels.

In Fig. 7 we present a comparison between the levels observed in our (p,t) reaction experiment and the prediction of the Interacting Boson Model-1 with s, p, d and f bosons (spdf-IBM-1) [12]. The parameters of these calculations are given in Ref. [7], where predictions of such calculations were compared with experimental data for both ^{166}Er and ^{168}Er. The two-neutron transfer intensities for the 0^+ states was also calculated for both these nuclei; while for ^{166}Er it is described reasonably well, the experimental features for ^{168}Er, consisting of a strong increase of the cumulative 0^+ transfer strength around 2.7 MeV is not well described (see Fig. 9 of [7]). Other transfer intensities were not calculated, because realistic 2n-transfer operators within this model contain a large number of parameters for each transferred L-value. In Fig.7 one can see that at higher excitation energies (above $\sim$ 2.5 MeV), the number of calculated states drastically underestimates that of the experimental observed states, for all J^π values evidenced in our (p,t) reaction study. It is likely that for the calculations with the QPM [10] and PSM [11] of other states than 0^+ and 2^+ this discrepancy for the number of states is smaller. The description of the 2n-transfer intensities remains, nevertheless, a particularly difficult issue for this nucleus. As observed in [2], the distribution of the 0^+ transfer intensity with excitation energy in ^{168}Er differs from that of the other eight nuclei from the rare-earth region. It is also different from that observed in its neighbour ^{166}Er [7]. The spdf-IBM calculations describe reasonably well the strong increase of this transfer intensity around 1.8 MeV in ^{166}Er, while they fail to describe the increase around 2.8-3.0 MeV from ^{168}Er [7].

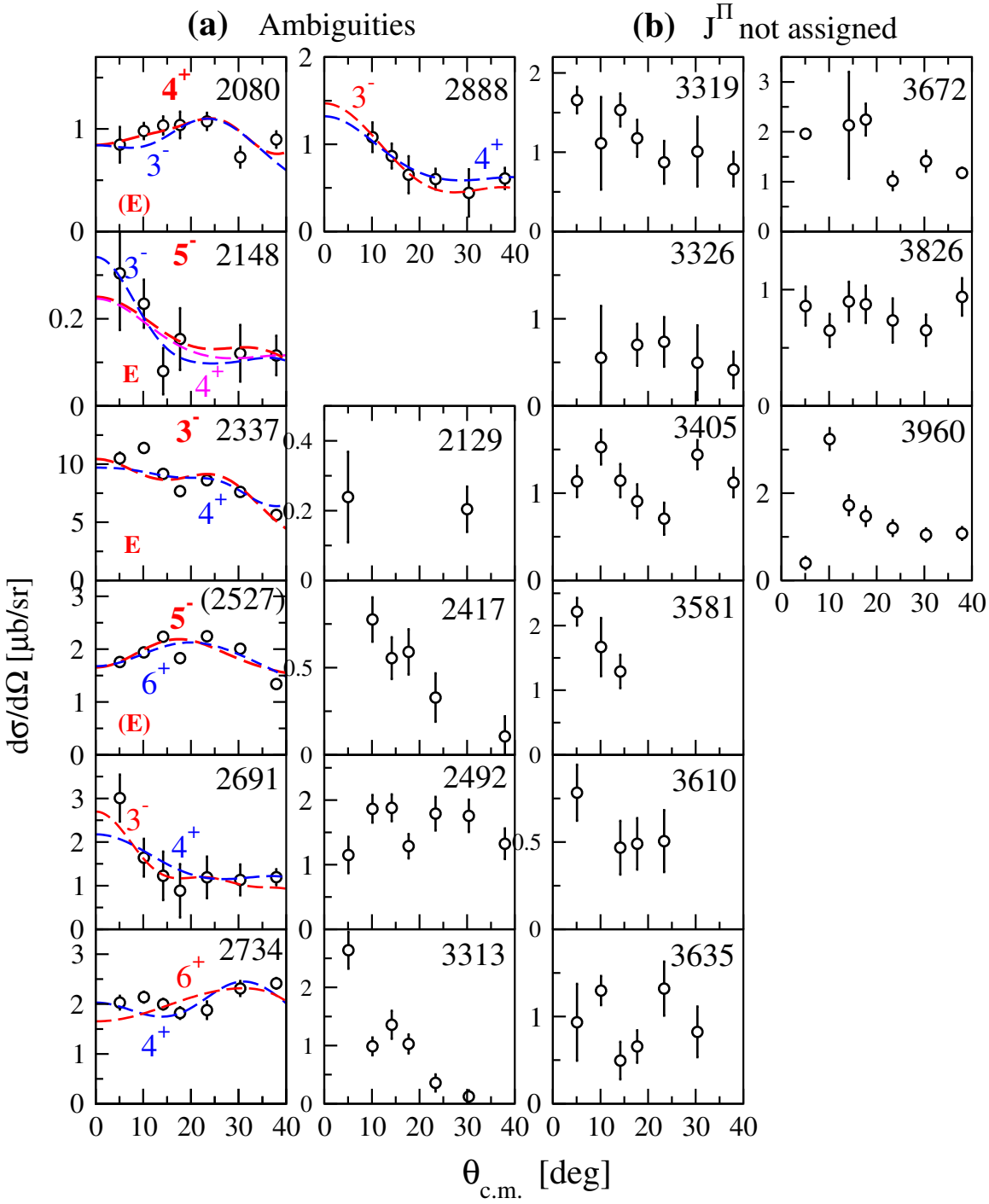

FIG. 6. (a) Some cases from our analysis where more than one J^π could be assigned to a certain state. For the first four states one of our possible assignments (marked in bold red number) coincides with the value adopted by ENSDF on the basis of other data. See also the discussion in the text. (b) Remaining states for which J^π values could not be assigned in this study.

^{168}Er is known as a deformed nucleus. Fig. 8 displays the excitation energies of the states observed in our study as a function of $J(J+1)$, a representation that evidences rotational bands as straight lines. In such a plot, states assigned to a band must be placed on a straight line and, in addition, the intensity of their population in the reaction (here taken as the integrated cross-sections from Table I) should decrease with increasing spin. The known bands at lower energies, resulting from previous studies, five for each parity, were clearly observed. In Fig. 8 they are labeled by the (red) capital letters used also in Ref. [9] (**A** to **K**. Some other bands are proposed (a few of

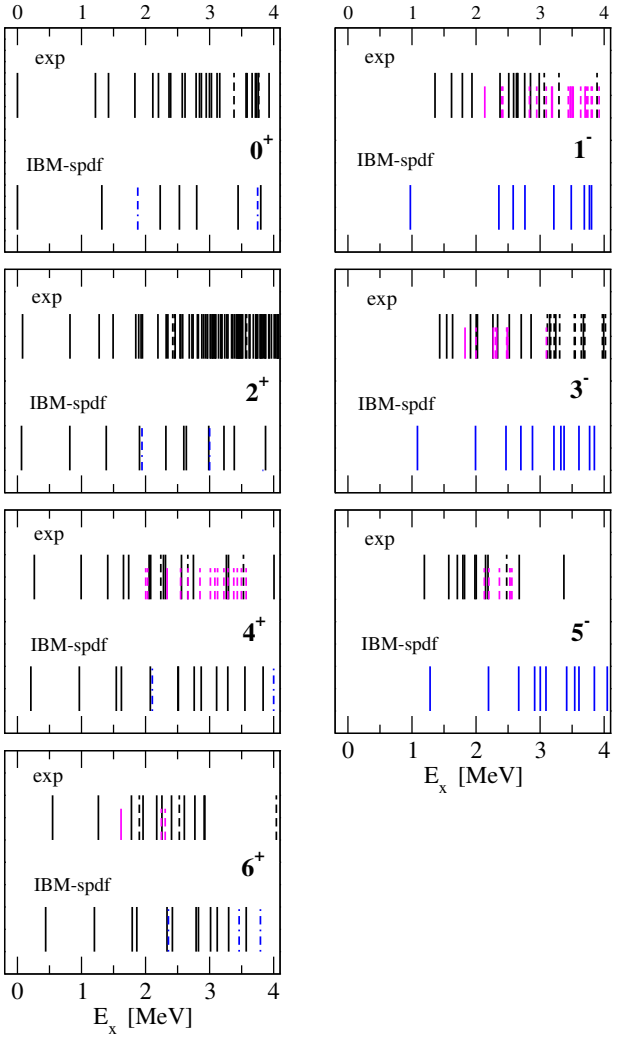

FIG. 7. Comparison between experimental states and states calculated by spdf-IBM-1. Esxperimental states: solid/dashed longer lines denote firm/tentative assignment of states obsered in this experiment, and shorter magenta lines with the same convention are states listed in ENSDF not observed in our experiment. The spdf-IBM-1 calculated states: dashed-dotted lines denote the two-octupole states.

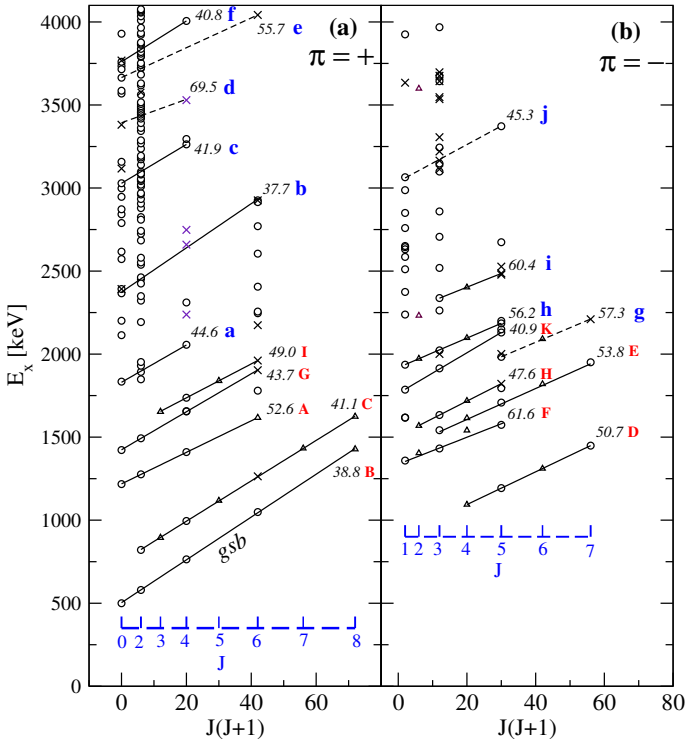

FIG. 8. Collective bands in ^{168}Er observed in this (p,t) reaction experiment (see also text). The states with firm/tentative spin assignment (Table I) are represented by circles/X's, respectively. The two known lowest 8^+ states are shown, although not observed in this experiment. For the bands with $K\neq 0$, the states of unnatural parity, most of them not observed in this experiment, have been added (when known [9]) as small triangles. For each identified band, the straight line shows the fit with the rotational formula, and its moment of inertia – MoI (in units $\hbar^2$MeV^{-1}) is given in the upper part of the line. The letters next to the MoI values have the following meaning. The capital (red) letters indicate the known bands labeled by that letter in [9]. The bands proposed on the basis of the present data are labeled by small (blue) letters (see the text for their identification). Note that the ground state band (gsb) was shifted up by 500 keV.

them tentatively) on the basis of the states observed in our reaction. In Fig. 8 they are labeled with (blue) small letters (**a** to **j**). These bands are as follows (see also Table I).

For the positive parity states (part (a) of the figure): *band a*, energy in keV and (J^π): 1834(0^+), 1893 (2^+), 2056 (4^+); *band b*: 2366 (0^+), 2462 (2^+), 2659 (4^+), and 2926 (6^+); *band c*: 3029 (0^+), 3081 (2^+), 3263 (4^+); *band d* (tentative): 3381 (0^+), 3442 (2^+), 3529 (4^+); *band e* (tentative): 3664 (0^+), 3729 (2^+), 4042 (6^+); *band f*: 3760 (0^+), 3838 (2^+), 4006 (4^+).

For the negative parity states (part (b) of the figure): *band g* (tentative): 1983 (5^-), 2091 (6^-), 2210 (7^-); *band h*: 1936 (1^-), 2022 (3^-), 2185 (5^-); *band i*: 2337 (3^-), 2402 (4^-), 2486 (5^-); *band j* (tentative): 3065 (1^-), 3165 (3^-), 3372 (5^-);

All the rotational bands in Fig. 8 are labeled with the value of the moment of inertia (derived from the slope of the straight lines from fits with the rotational model formula), in units $\hbar^2$MeV^{-1}. The ground state band (gsb) has a moment of inertia of 38.8 $\hbar^2$MeV^{-1}, which is practically 50% of a rigid-body ellipsoid having the quadrupole deformation $\beta_2 = 0.31$ of ^{168}Er [9]. For the positive-parity bands the moment of inertia values in Fig. 8 are relatively well grouped close to the value of the gsb. For the negative-parity bands the values observed are, on average, somewhat larger than those of the positive-parity bands. Due to the relatively small number of bands assigned from the present data, one cannot deduce trends of the behaviour of the moment of inertia values with the excitation energy.

VI. CONCLUSIONS

In this work, a complete analysis of the states observed in the ^{170}Er(p,t) reaction at an incident energy of 25 MeV has been reported. This reaction populated with measurable cross-section a number of about 220 excited states up to an excitation energy of 4075 keV. In order to assign J^π values to these states, the large variety of observed angular distribution shapes was analysed with coupled channel calculations performed with the code CHUCK3, according to four different multistep coupled channel schemes (Fig. 1). For a large number of the excited states, the J^π values assigned by our study (Table I) corroborated those from independent studies evaluated for the ENSDF database [9]. The coupled channel calculations prove a strong instrument for the characterization of the states populated in this 2n-transfer reaction. There is a reserve that in some cases one may be in a situation of unambiguous assignment of the transferred L value.

With the new J^π determinations from this work for more than 100 excited states, ^{168}Er remains one of the best characterized nuclei below 4 MeV excitation, and thus represents a challenge for future microscopic theoretical nuclear structure models. It is difficult, however, to appreciate how "complete" is the level scheme of this nucleus for different spins and parities, especially in the region of high-level density above 3 MeV.

[1] D.A. Meyer, V. Wood, R.F. Casten, C.R. Fitzpatrick, G. Graw, D. Bucurescu, J. Jolie, P. von Brentano, R. Hertenberger, H.-F. Wirth, N. Braun, T. Faestermann, S. Heinze, J.L. Jerke, R. Krücken, M. Mahgoub, O. Möller, D. Mücher, C. Scholl, Phys. Lett. B **638** 44 (2006).

[2] D.A. Meyer, V. Wood, R.F. Casten, C.R. Fitzpatrick, G. Graw, D. Bucurescu, J. Jolie, P. von Brentano, R. Hertenberger, H.-F. Wirth, N. Braun, T. Faestermann, S. Heinze, J.L. Jerke, R. Krücken, M. Mahgoub, O. Möller, D. Mücher, C. Scholl, Phys. Rev. C **74** 044309 (2006).

[3] D. Bucurescu, G. Graw, R. Hertenberger, H.-F. Wirth, N. Lo Iudice, A.V. Sushkov, N.Yu. Shirikova, Y. Sun, T. Faestermann, R. Krücken,M. Mahgoub, J. Jolie, P. von Brentano, N. Braun, S. Heinze, O. Möller, D. Mücher, C. Scholl, R.F. Casten, D.A. Meyer, Phys. Rev. C **73**, 064309 (2006).

[4] A. I. Levon, G. Graw, Y. Eisermann, R. Hertenberger, J. Jolie, N. Yu. Shirikova, A. E. Stuchbery, A. V. Sushkov, P. G. Thirolf, H.-F. Wirth, and N. V. Zamfir, Phys. Rev. C **79**, 014318 (2009).

[5] A. I. Levon, G. Graw, R. Hertenberger, S. Pascu, P.G. Thirolf, H.-F. Wirth, and P. Alexa, Phys. Rev. C **88**, 014310 (2013).

[6] A.I. Levon, D. Bucurescu, C. Costache, T. Faestermann, R. Hertenberger, A. Ionescu, R. Lica, A.G. Magner, C. Mihai, R. Mihai, C.R. Nita, S. Pascu, K.P. Shevchenko, A.A. Shevchuk, A. Turturica, and H.-F. Wirth, Phys. Rev. C **100**, 034307 (2019); Phys. Rev. C **102**, 014308 (2020).

[7] D. Bucurescu,S. Pascu, G. Suliman, H.-F. Wirth, R. Hertenberger, T. Faestermann, R. Krücken, and G. Graw, Phys. Rev. C **100**, 044316 (2019).

[8] P. D. Kunz, Computer code CHUCK3, University of Colorado (unpublished).

[9] C.M. Baglin, Nuclear Data Sheets **111**, 1807 (2010).

[10] V. G. Soloviev, *Theory of Atomic Nuclei: Quasiparticles and Phonons* (Institute of Physics, Bristol, 1992).

[11] K. Hara and Y. Sun, Int. J. Mod. Phys. E **4**, 637 (1997).

[12] F. Iachello and A. Arima, *The Interacting Boson Model* (Cambridge University Press, Cambridge, 1987).